Proceedings World Geothermal Congress 2026, Calgary, Canada, June 8—11, 2026

Unlocking Nigeria's Geothermal Energy Potential: Insights from High-Resolution Aeromagnetic and Aero-Radiometric Data

Ikechukwu, Chigozie Chukwuemeka[1*], Ezekiel, Chima Justin[2], Opara, Alexander Iheanyichukwu[3]

[1*,2]Department of Earth, Energy & Environment, University of Calgary, 2500 University Drive NW, T2N 1N4, Calgary, Alberta, Canada
[1*,3]African Centre of Excellence in Future Energies and Electrochemical Systems (ACE-FUELS), Federal University of Technology, P.M.B 1526, Owerri, Nigeria
chigozie.ikechukwu@ucalgary.ca; ikechukwuchigoziechukwuemeka@gmail.com

INTRODUCTION

Nigeria's Energy Transition Plan (2022) champions renewable energy to achieve SDGs 7 & 13. While studies have highlighted its potential (Ekpotu et al., 2024; Emmanuel et al. 2025), geothermal energy remains a significantly **under-explored resource**.

This study presents an assessment of Nigeria's geothermal potential across strategic regions, including the Benue Trough and Younger Granite provinces. Applying spectral inversion on high-resolution aeromagnetic data and radiogenic heat production (RHP) estimation from high-resolution aero-radiometric data, we calculated key indicators:

- **Curie Point Depth (CPD)**
- **Geothermal Gradient**
- **Heat Flow**

} Derivatives of Spectral Inversion of aeromagnetic geophysical data

- **Radiogenic Heat Production** } Derived from aero-radiometric Geophysical data

Our findings reveal **exceptionally high heat flow and shallow heat sources**, far exceeding typical continental values. This confirms significant potential for both electricity generation and direct-use applications. This work provides a critical foundation to guide future exploration and investment, accelerating Nigeria's transition to a sustainable energy future.

METHODS

The estimation of the heat flow was derived from spectral analysis of magnetic data, following an established geophysical method:

1. **Data Processing:**

i. The Total Magnetic Intensity (TMI) grid was first processed to isolate the magnetic signature of deep-seated sources. A regional-residual separation was performed to remove long-wavelength anomalies, resulting in a Residual Magnetic Intensity (RMI) map ***(Blakely, 1996)*** .

ii. RMI map was then transformed using Reduction to the Magnetic Equator (RME), a crucial correction that repositions magnetic anomalies directly above their source bodies. ***(Baranov, 1957; Mendonça and Silva, 1993)***

2. **Spectral Analysis:** The RMI data was partitioned into overlapping windows for 2D spectral analysis. The depth to the top of the magnetic sources and the Centroid depth were calculated from the slope of the energy spectrum within each window ***(Spector and Grant, 1970; Okubo et al., 1985)*** .

3. **Curie Point Depth (CPD) Calculation:** The basal depth of the magnetic source, interpreted as the Curie Point Depth (CPD) where rocks lose their ferromagnetic properties (~580°C for magnetite), was calculated from the estimated depth parameters ***(Tanaka et al., 1999).***

4. **Geothermal Gradient Derivation:** Finally, the geothermal gradient was calculated by assuming the Curie temperature is isothermal and using the standard heat flow equation, where Heat Flow is a function of the thermal gradient and thermal conductivity ***(Turcotte and Schubert, 2002)*** .

RADIOGENIC HEAT PRODUCTION

The radiogenic heat production (RHP) of rocks was quantitatively estimated using the empirical formula established by **Rybach (1976)**. This method calculates the amount of heat generated within the crust due to the natural radioactive decay of specific elements.

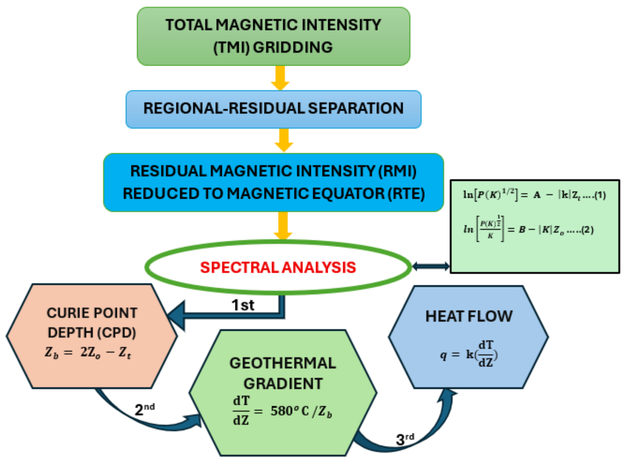


Fig. 1: CPD, Geothermal Gradient and Heat Flow Flowchart Methodology

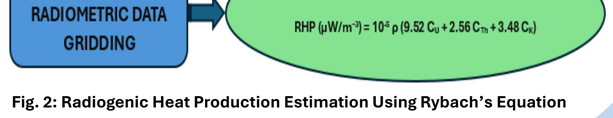


Fig. 2: Radiogenic Heat Production Estimation Using Rybach's Equation

RESULTS

Table 1. CPD, Geothermal Gradient, Heat Flow, and RHP

Block_ID	Zt_Top_Depth km	Zo_Centroid_Depth _km	Zb_Curie_Depth _km	Geothermal_ Gradient_ °C/km	Heat_Flow_ mW/m2	RHP_MEAN (μW/m³)
B1	0.223833355	9.098187118	17.97254088	32.27145254	80.6786313	0.00201
B2	0.211051406	9.702488238	19.19392507	30.21789435	75.5447359	0.00214
B3	0.20607275	9.54005026	18.87402777	30.73005969	76.8251492	0.00222
B4	0.216120417	9.063609664	17.91109891	32.38215605	80.9553901	0.00221
B5	0.277975121	8.412286668	16.54659822	35.05252212	87.6313053	0.00223
B6	0.206720596	7.715582419	15.22444424	38.09662874	95.2415718	0.00242
B7	0.231827227	9.269487863	18.3071485	31.68161334	79.2040333	0.00211
B8	0.19568875	9.83473888	19.47378901	29.7836235	74.4590588	0.00203
B9	0.203853285	9.277356154	18.35085902	31.60614984	79.0153746	0.00206
B10	0.221785568	8.01254698	15.80330839	36.70117583	91.7529396	0.00213
B11	0.223900938	7.533862584	14.84382423	39.07348881	97.683722	0.00222
B12	0.210352306	8.446469992	16.68258768	34.76678865	86.9169716	0.00207
B13	0.210999789	9.103424247	17.99584871	32.22965527	80.5741382	0.00204
B14	0.224278427	10.20399852	20.18371861	28.7360328	71.840082	0.00208
B15	0.110780555	9.570892848	19.03100514	30.47658259	76.1914565	0.00226
B16	0.217731914	8.933726924	17.64972193	32.86170752	82.1542688	0.00197
B17	0.221001783	9.506908146	18.79281451	30.86285983	77.1571496	0.00162

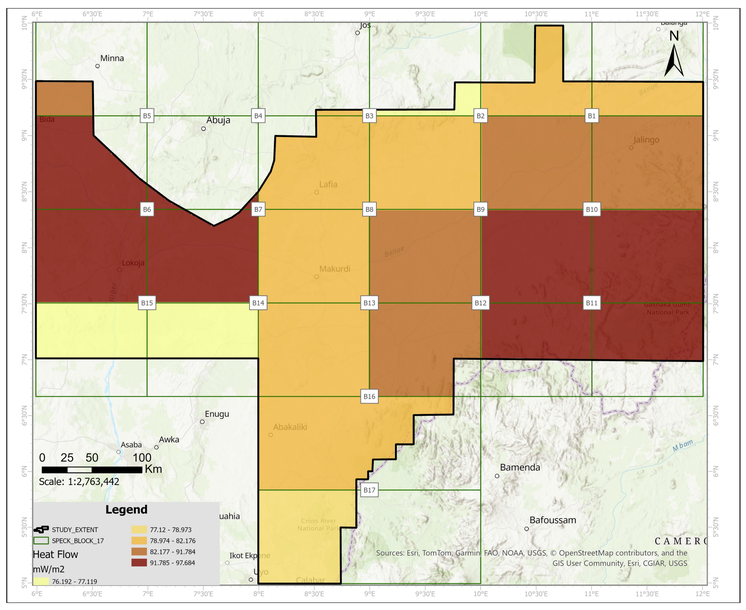
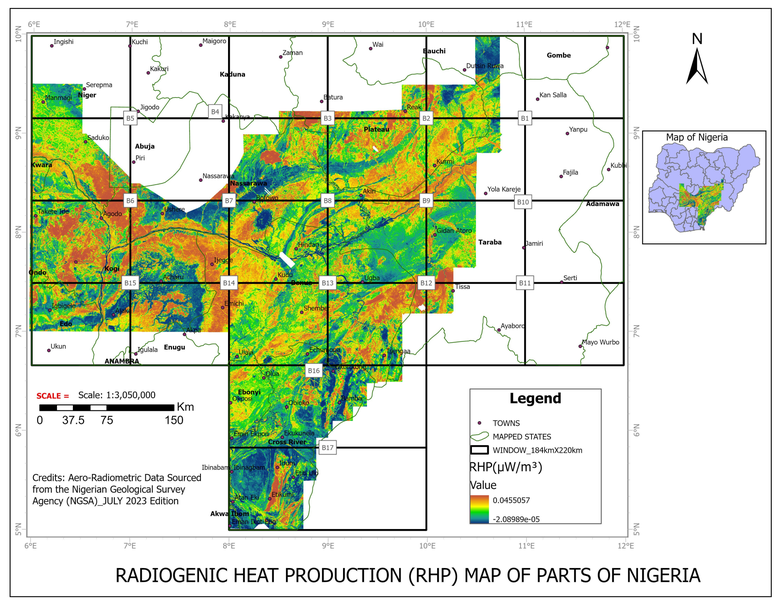


Fig. 3: HEAT FLOW MAP OF THE STUDY AREA



RADIOGENIC HEAT PRODUCTION (RHP) MAP OF PARTS OF NIGERIA

Fig. 4: RHP MAP OF THE STUDY AREA

Analysis of the 17 blocks reveals a distinctly heterogeneous thermal regime, with heat‑flow values ranging from approximately 71 to 98 mW/m² and geothermal gradients from about 28 to 39 °C/km. Blocks B11, B6 and B10 stand out as the most thermally anomalous areas, combining the highest geothermal gradients (>36 °C/km), highest heat‑flow values (>91 mW/m²) and the shallowest Curie Point Depths (CPD ≈ 14.8–15.8 km). In contrast, blocks such as B14 and B8 show lower geothermal gradients (<30 °C/km), comparatively deep CPDs (>19 km) and reduced heat flow (~72–75 mW/m²), indicating a cooler, less prospective crust.

The spatial distribution of heat flow defines a west–east belt of elevated values that mirrors the structural grain and magmatic history of the Benue Trough and adjoining basement. High heat flow blocks in the west (e.g. B5–B6) align with the southern Bida Basin and the western termination of the Middle Benue, while the strongest anomaly in the East (B11) coincides with the structurally complex Middle–Upper Benue sector. Overall, blocks with geothermal gradients exceeding ~35 °C/km (B5, B6, B10, B11) consistently exhibit heat flow values above ~87 mW/m², confirming a robust inverse relationship between CPD and surface thermal output.

A moderate positive correlation is observed between heat flow and Radioactive Heat Production (RHP), with a Pearson correlation coefficient of $r=0.42$. Although mean RHP values are generally low (~0.002 μW/m³), block‑scale variations are meaningful: B6 records both the highest mean RHP (0.00242 μW/m³) and one of the highest heat‑flow values (95.24 mW/m²), whereas B17, with the lowest RHP (0.00162 μW/m³), corresponds to a relatively lower heat flow (77.16 mW/m²). These relationships suggest that RHP contributes measurably to the heat budget but does not solely control the observed anomalies.

DISCUSSION

•Shallow CPD, high geothermal gradients and elevated heat flow in the study area point to a predominantly tectono-magmatic control on the thermal regime, consistent with earlier work in the Benue Trough (Anakwuba et al., 2019; Ofoegbu & Onuoha, 1991; Nwankwo et al., 2011).

•The hottest blocks (B11, B6, B10) coincide with structurally complex segments of the Benue Trough and adjacent basins, previously mapped as zones of crustal extension, intrusive magmatism and high lineament density, supporting a model of crustal thinning and felsic intrusions elevating isotherms and enhancing heat transfer (Ofoegbu, 1985; Onwuemesi, 1997; Anakwuba et al., 2019).

•A moderate correlation between RHP and heat flow indicates that radiogenic heat is a secondary but non-negligible source: more radiogenic lithologies (e.g. granitic/felsic basement in B6) tend to higher heat flow, yet high anomalies also occur where RHP is modest, implying a dominant contribution from mantle heat input and structurally focused flow (Nyabeze & Gwavava, 2016; Bello et al., 2023; Anakwuba et al., 2019).

•The contrast between shallow CPDs in hot blocks (e.g. B11, B6, B10) and deeper CPDs in cooler blocks such as B14 emphasizes the primary role of crustal structure and thickness, rather than composition alone, in controlling the regional geothermal field (Oladunjoye et al., 2017; Anakwuba et al., 2019).

•Exploration results define a clear geothermal hierarchy: B11, B6 and B10, with gradients well above the global continental average of 25–30 °C/km and heat-flow levels comparable to known geothermal provinces, are prime targets for high-enthalpy resource assessment, including detailed geophysical surveys and temperature-gradient drilling (Pollack et al., 1993; Hurter & Haenel, 2002; Wygrala, 1989; Garg & Combs, 2015).

•Central and southern blocks with intermediate heat flow are better suited to direct-use applications such as space heating and agro-processing, where moderate temperatures are adequate and drilling costs can be minimized (Lund & Freeston, 2001; Bromley et al., 2010).

•Cooler blocks (e.g. B14 and B8), though less favorable for power generation, provide an important thermal baseline and help delineate the lateral boundaries of the high-potential anomalies, refining the overall exploration strategy (Hurter & Haenel, 2002; Lund & Freeston, 2001).

CONCLUSION

•**Integrated Exploration Framework**: This research demonstrates that combining Curie Point Depth (CPD), geothermal gradient, heat-flow estimates, and Radioactive Heat Production (RHP) creates a powerful framework for identifying geothermal targets in regions with limited data.

•**Identification of High-Heat Belt**: The analysis reveals a continuous, structurally controlled high-heat-flow belt across the study area.

•**Primary Prospect Blocks**: Blocks B11, B6, and B10 are identified as first-order prospects for high-enthalpy geothermal exploration.

•**Geological Drivers**: The coincidence of shallow CPDs and high heat flow with the Benue Trough suggests that crustal thinning and magmatism are the primary drivers of the thermal regime, with radiogenic heat serving as a secondary enhancer.

•**Commercial Viability**: Prioritizing exploration in these thermally anomalous blocks provides the best opportunity to develop commercially viable resources for electricity generation and high-temperature industrial use.

Acknowledgements

We acknowledge the Nigerian Federal Government for its investment in acquiring the high-resolution aeromagnetic and aeroradiometric data used in this study. We are also grateful to the Ministry of Mines and Steel Development (MMSD) and the Nigerian Geological Survey Agency (NGSA) for making these data publicly available.

REFERENCES

Baranov, V. (1957). Interpretation des anomalies gravimetriques quelques developpements recents. *Bulletin Géodésique (1946-1975)*, *45*(1), 20-25.

Blakely, R. J. (1996). *Potential theory in gravity and magnetic applications*. Cambridge university press.

Ekpotu, W., Akintola, J., Moses, Q., Obialor, M., Osagie, E., Utoh, I. O., & Akpan, J. (2024, August). Nigeria's Energy Transition Plan: A Technical Analysis, Opportunities, and Recommendations for Sustainable Development. In *SPE Nigeria Annual International Conference and Exhibition* (p. D032S030R007). SPE.

Emmanuel, P. M., Tidi, M. E., & Akanni, Y. I. (2025). Energy transition and environmental sustainability in developing economies: insights from Nigeria's policy landscape towards achieving SDGs 7 and 13. *Environment, Development and Sustainability*, 1-25.

Mendonça, C. A., & Silva, J. B. (1993). A stable truncated series approximation of the reduction-to-the-pole operator. *Geophysics*, *58*(8), 1084-1090.

Okubo, Y., Graf, R. J., Hansen, R. O., Ogawa, K., & Tsu, H. (1985). Curie point depths of the island of Kyushu and surrounding areas, Japan. *Geophysics*, *50*(3), 481-494.

Rybach, L. (1976). Radioactive heat production in rocks and its relation to other petrophysical parameters. *Pure and Applied Geophysics*, *114*(2), 309-317.

Spector, A., & Grant, F. S. (1970). Statistical models for interpreting aeromagnetic data. *Geophysics*, *35*(2), 293-302.

Tanaka, A., Okubo, Y., & Matsubayashi, O. (1999). Curie point depth based on spectrum analysis of the magnetic anomaly data in East and Southeast Asia. *Tectonophysics*, *306*(3-4), 461-470.